J. Fish. Sci. Tech. 1(2), 260~268, 1998

Hydraulic Model Experiment on the Circulation in Sagami Bay, Japan (III)

– The Time-Varying States of the Flow Pattern and Water Exchange in Barotropic Rotating Model –

Hyo-Sang Choo* and Takasige Sugimoto[1]

Dept. of Oceanography, Yosu National Univ., Korea [1]Ocean Research Institute, Univ. of Tokyo, Japan

(Received September 1998, Accepted December 1998)

A flow pattern and water exchange in Sagami Bay is examined using a barotropic hydraulic model. In the model experiments, the volume transports of the Kuroshio Through Flow were changed with time.

The results of the model experiments show that when the volume transport is increased with time, water mass and vorticity are transferred to the inner part of the bay by wakes from the western part of the bay. In the case of decrease, as the wakes are ceased, the inner cyclonic circulation water is discharged to the outside of the bay by its southward extension through theOshima eastern channel. It is found that the water exchange by the short-term variation of volume transport in time is about 20% of all the bay water.

Key words: Water exchange, time-varying flow pattern, barotropic rotating model, Sagami Bay

Introduction

Sagami Bay which is 80 kilometers wide and 5 kilometers long is an open-typed bay in the southwest of main island of Japan (Fig. 1). The entrance of the bay is divided into two parts by Oshima island. The western part named Oshima western channel is about 600 meters deep with its maximum depth at sill and 21 kilometers wide. The eastern part named Oshima eastern channel is about 2000 meters deep and 37 kilometers wide. There exists a current branched from Kuroshio which flows along the southern coast of Japan. The branch current - this current has been called by the Kuroshio Through Flow (hereafter KTF) - flows in Sagami Bay from Oshima western channel and flows out through Oshima eastern channel when the Kuroshio passes through the Izu-Ogasawara Ridge almost nomal to the direct path of the Kuroshio (Uda, 1937; Kawabe and Yoneno, 1987). The KTF from the Oshima western channel is intensified as the Kuroshio approaches Sagami Bay (Iwata and Matsuyama, 1989).

About the flow pattern in Sagami Bay, Uda (19 37) drew an average flow pattern based on the hydrographic field observation when the KTF flows into Oshima western channel. Kimura (1942), Yoshida (1960) and Kawata and Iwata (1957) identified the existence of the KTF and the cyclonic circulation in the inner part of the bay by tracking drifting buoys, GEK and current measurement. Tameishi (1988) showed the circulation patterns by using NOAA infrared images in Sagami Bay. Choo and Sugimoto (1992), Sugimoto and Choo (1992) and Kimura et. al. (1994) revealed that the flow pattern and the circulation structure were mostly affected by the fluctuation of the KTF from the both results of the field observation and the hydraulic model experiment.

Regarding the water exchange between the bay water and the KTF in Sagami Bay, Nakata and Hasunuma (1987) and Nakata et. al. (1989) examined the water exchange process between the coastal bay water and Kuroshio warm water (KTF) from the observations of drift buoys and drift cards at the frontal region where the KTF and the inner bay water were met with. It was found that a large horizontal velocity shear existed between the KTF and the inner cyclonic circulation and cyclonic and anticyclonic circulation modes were formed according to the variation of the KTF. They also suggested that the water exchange occured as the front fluctuated south and north. However, those observational results could not reveal the change

*To whom correspondence should be addressed.

process of the flow pattern quantitatively because the inflow conditions of the KTF were not studied during the observational periods.

It has been assumed that the water exchange and the change of the flow pattern in Sagami Bay are connected with various fluctuation periods and amplitudes in Kuroshio and the KTF at Oshima western channel. It is also assumed that various horizontal response and instability caused by coastal topography have been included in the change process of the flow pattern.

An experimental attempt using an hydraulic model has been known as one of the most effective means for studying the non-steady state process (Whitehead and Miller, 1979; Sugimoto and Choo, 1992) and it is suggested that an hydraulic model experiment will be effective to understand the water exchange and the change of the flow pattern by the fluctuation of the KTF in Sagami Bay (Choo and Sugimoto, 1999).

The purpose of our hydraulic model experiment is to examine the change process of the flow pattern and the water exchange in Sagami Bay by the fluctuation of the KTF. For this purpose, barotropic model experiments were executed. In model experiments, various parameterization was attempted. Time-varying states of the flow pattern and the water exchange were fully reproduced by changing the inflow with time.

Models and Experimental Arrangement

Basic equations and similitude

Supposing that a depth change of the flow layer would not have influence so much on the phenomena to be examined, a vorticity equation with a constant depth was used in model experiments as a basic governing equation (Choo and Sugimoto, 1992).

$$\partial\zeta/\partial t+V\cdot\nabla\zeta=K_h\nabla^2\zeta-(f\cdot K_z)^{1/2}\zeta/H \qquad (1)$$

where ζ is the vertical component of relative vorticity ($\zeta=k\cdot(\nabla\times V)$), k is the unit vector in vertical direction, V is the horizontal velocity vector, t is time, $\nabla=i\,\partial/\partial x+j\,\partial/\partial y$, $\nabla^2=\partial^2/\partial x^2+\partial^2/\partial y^2$, H the typical thickness of the flow layer, f the Coriolis parameter, K_h and K_z the horizontal and the vertical eddy viscosity, respectively. Equation (1) for the prototype can be scaled with L the typical horizontal length scale (45 km), f^{-1} the typical time scale, V_0 the characteristic speed of the KTF at Oshima western channel and H_0 (200 m) the characteristic value of H. Substituting ζ for $V_0/L\cdot\zeta^*$, then equation (1) becomes

$$\partial\zeta^*/\partial t^*+(V_0fL)_p V^*\cdot\nabla^*\zeta^*=(K_hfL^2)_p\nabla^2\zeta^*-(K_z/fH_0^2)_p^{1/2}\zeta^*/H^* \qquad (2)$$

where asterisks mean non-dimensional variables, and suffix p denotes prototype. Non-dimensional parameter V_0/fL indicates Rossby number (Ro), K_h/fL^2 horizontal Ekman number (Ek_h), K_z/fH_0^2 vertical Ekman number (Ek_z), respectively. Using the value $K_h\sim1.8\times10^5$ cm^2/s and $K_z\sim2.6\times10$ cm^2/s, the values of non-dimensional parameters in equation (2) become $Ro\sim10^{-1}$, $Fr_i\sim10^{-1}$, $Ek_h\sim10^{-4}$ and $Ek_z\sim10^{-4}$ as shown in Table 1.

Therefore, the non-dimensional vorticity equation for the model is

$$\partial\zeta^*/\partial t^*+(V_0/2\Omega L)_m V^*\cdot\nabla^*\zeta^*=(\nu/2\Omega L^2)_m\nabla^2\zeta^*-(\nu/2\Omega H_0^2)_m^{1/2}\zeta^*/H^* \qquad (3)$$

where ν is the molecular viscosity, Ω the angular velocity of the turntable and the suffix m denotes model, respectively. If non-dimensional parameters in equations (2) and (3) are equal to each other, the flow patterns in the prototype and the model will be equivalent. That is ;

$$[V_0/fL]_p=[V_0/2\Omega L]_m \qquad (4)$$
$$[K_h/fL^2]_p=[\nu/2\Omega L^2]_m \qquad (5)$$
$$[K_z/fH_0^2]_p=[\nu/2\Omega H_0^2]_m \qquad (6)$$

Each ratio Vr, Lr, Hr and Tr represents $Vr=(V_0)_p/(V_0)_m$, $Lr=(L)_p/(L)_m$, $Hr=(H_0)_p/(H_0)_m$ and $Tr=2\Omega/f$ respectively. From equation (4)~(6), $Vr=Tr^{-1}Lr$, $Lr=(TrK_h)^{1/2}$ and $Hr=(TrK_z)^{1/2}$. As Lr and Hr

Table 1. Scale ratios of the model and the values of parameters for the prototype and the model.

Property		Scale ratio	Prototype	Model
Horizontal length	L	$L_r=3.0\times10^5$	45 km	15 cm
Vertical length	H	$H_r=3.6\times10^3$	1000 m	28 cm
Time	T	$T_r=5.0\times10^3$	1.5×10^5 sec	30 sec
Volume transport	Q	$Q_r=6.5\times10^{10}$	2.0×10^{12} cm^3/s	30 cm^3/s
Velocity	V	$V_r=6.0\times10^1$	60 cm/s	1.0 cm/s
Kinematic	K_h	$K_{hr}=1.8\times10^7$	1.8×10^5 cm^2/s	0.01 cm^2/s
Viscosity	K_z	$K_{zr}=2.6\times10^3$	2.6×10^1 cm^2/s	0.01 cm^2/s

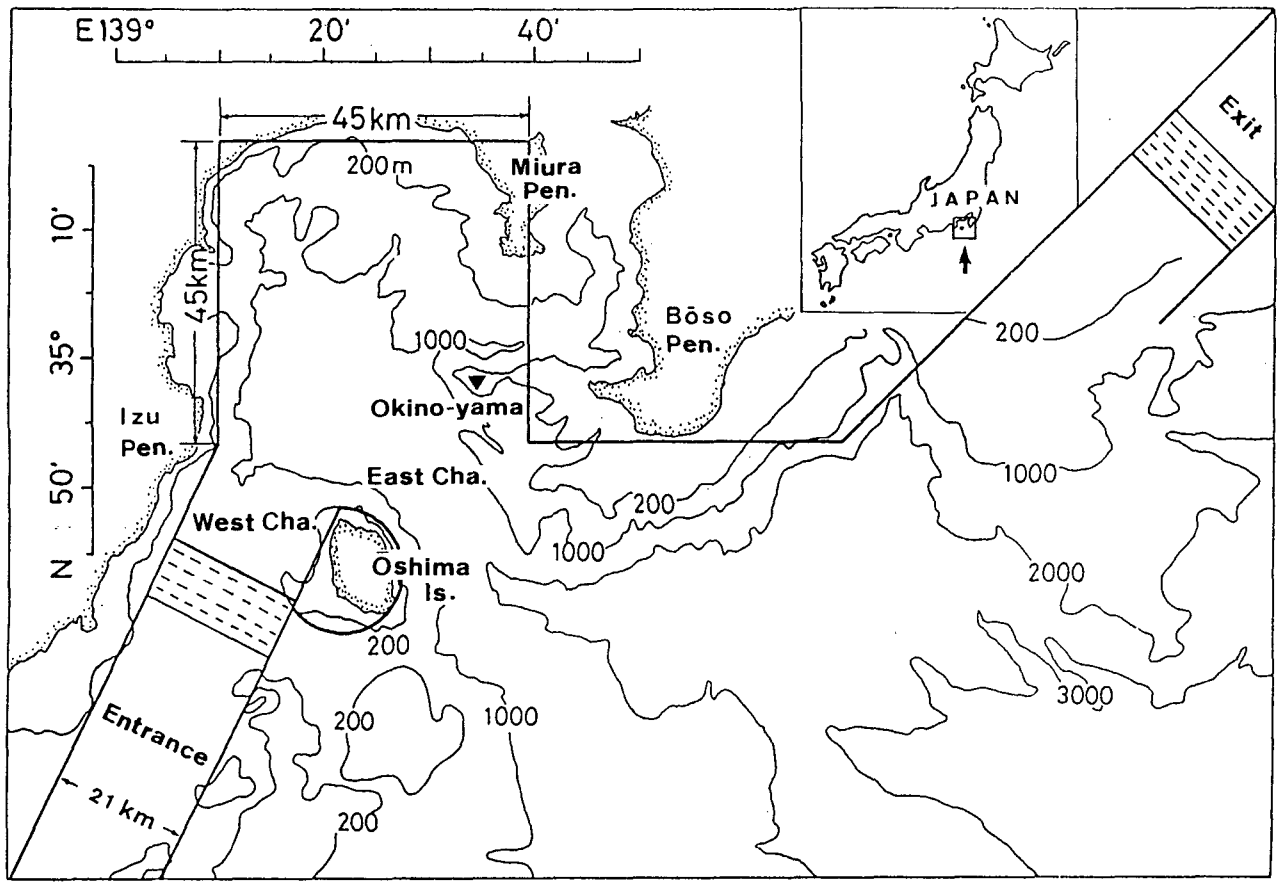

Fig. 1. Domain of the hydraulic model and the general configuration. Thin lines show bathymetry of the prototype.

are depended on angular velocity Ω, Lr and Hr are determined within the range of the given angular velocity. However, in order to estimate Lr and Hr the values of Kh, Kz and should be known. The molecular viscosity ν for water has the value of 10^{-2} cm^2/s generally. The values of K_h and K_z in prototype were determined to be satisfied with their practical order (Choo and Sugimoto, 1992). Volume transport (flow rate) ratio Qr is calculated by $Qr = VrHrLr = Lr^2HrTr^{-1}$. A typical set of these scale ratios is listed in Table 1. The depth of 5.5 cm was adopted as the mean water depth of the model, which corresponded to the 200 m depth of the flow layer in the prototype.

Experimental facilities and procedure

A general geometry of Sagami Bay and domain of the hydraulic model were shown in Fig. 1. Fig. 2 (a) and (b) show the side views of the model used in experiments, its outside arrangement and the measurement system, respectively. The model basin has 35 cm height, 120 cm width and 80 cm length. Fresh water which has 5.5 cm depth in the model is injected from the entrance channel (source) to the exit channel (sink) by use of electro-magnetic pumps and floater-type flow meters. Turbulence from the source and the sink was reduced by screens, iron nets and sponges.

According to the six-days current observation in Oshima western channel (Taira and Teramoto, 19 86), the volume transport of the KTF from Oshima western channel fluctuated from 1.5 Sv to 2.1 Sv with the mean value of 1.8 Sv. It was also found that the volume transport of the KTF had the range of 0.5 Sv~4.0 Sv (Taira and Teramoto, 1981). Therefore, time variations of volume transport in the model experiments were given by three cases, i. e., the small (0.4~0.9 Sv), the middle (1.4~1.8 Sv) and the large (2.7~3.2 Sv). The volume transport (flow rate) was changed from 6.6 cc/s to 8.5 cc/s (0. 4~0.5 Sv in prototype) for one rotation of the turn table (1.7 days in prototype). Fig. 3 shows the time variation of volume transport in the model experiments. Experimental cases and parameter

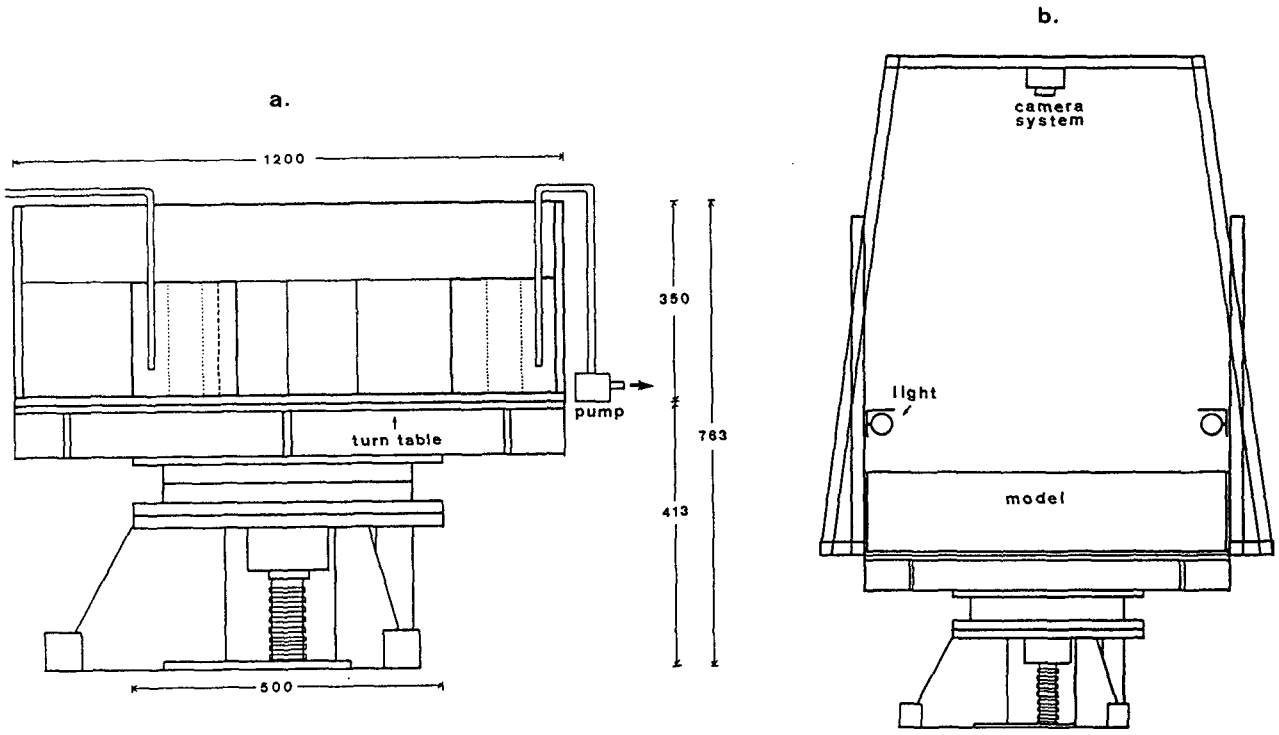

Fig. 2. (a) Schematic views of the turntable, the tank and (b) the measurement system in the model experiment. All dimensions are given in millimeters.

ranges for the variation of volume transport in the model were listed in Table 2.

Minute process of the flow changes due to the time variations of volume transport was determined by use of photography and video tapes. Water particles which were visualized by tracing the motion pictures on video tapes were tracked and trajectories were drawn at selected 11~12 points in the model bay. The amount of water exchange between the bay water and the KTF water was estimated by calculating the surface area of each water.

Results and discussion

Variations of flow patterns with flow rate change

Response of flow pattern to the variation of injected water mass (flow rate) is a non-steady state process in the balance of mass and force added to the basic flow field. Choo and Sugimoto (1992) studied the flow patterns of the bay in steady state and reported that the wakes and the boundary conditions of the flow should be taken into account for estimating the flow field in Sagami Bay. Their results suggest that the behaviour of the wakes and their interaction with the KTF are very important to investigate the change process of the flow pattern in Sagami Bay.

In order to examine the variations of the flow patterns by the fluctuations of the KTF, experiments for flow rate changes were executed. Fig. 4 (a)~(c) and Fig. 5 (a)~(c) show the variations of the northern (outside) edges of the KTF at intervals of 30 seconds after the flow rates were increased and decreased in a small flow rate range (5.5~14.0 cc/s), respectively. The northern edge of the KTF

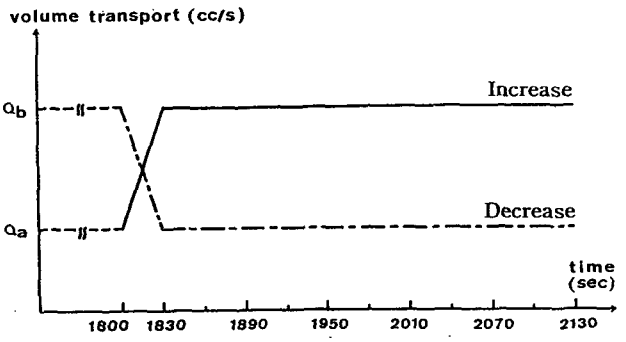

Fig. 3. Time variations of volume transport in the model experiments. "Increase" and "Decrease" in the figure represent increase and decrease of the injected fresh water at the entrance channel, respectively.

Table 2. Cases and parameter ranges for the time variance in the model experiments

Factors	Values given in the model			
Revolution rate	Ω (rpm)	2		
Volume transport	Q (cc/s)	5.5~14.0	20.8~27.0	42.0~48.6
Volume transport change	ΔQ (cc/s)	8.5	6.2	6.6

was determined by tracing the minute motion of the KTF in the model.

30 seconds later (Fig. 4 (a)), the northern edge of the KTF is widely extended to northwest. At this moment, some parts of the cyclonic circulation (Choo and Sugimoto, 1992) near the northwest of the bay are trapped in the west of the bay. However, 60 seconds later, the KTF path conversely comes down more to south than before the flow rate is increased. 90 seconds later, cyclonic eddies are formed at the westward entrance of the bay. 120~150 seconds later (Fig. 4 (b)), as the eddies are continuing to grow, they move to the middle of the bay and then, the KTF path begins to penetrate into the bay. However, 180 seconds later the KTF path advances southward and does not show any remarkable changes. While, the northern edge of the KTF near the eastern boundary of the bay is not changed so much till 180 seconds but generally changed 210 seconds later. The KTF path in the eastern boundary of the bay goes down to south with time.

In Fig. 5 (a), (b) and (c), branches take place in the KTF path from the beginning of the flow rate decrease till 30~60 seconds. 60 seconds later (Fig. 5 (a)), the coastal waters of the cyclonic circulation which have been extended down at the western boundary are transferred below the branched path

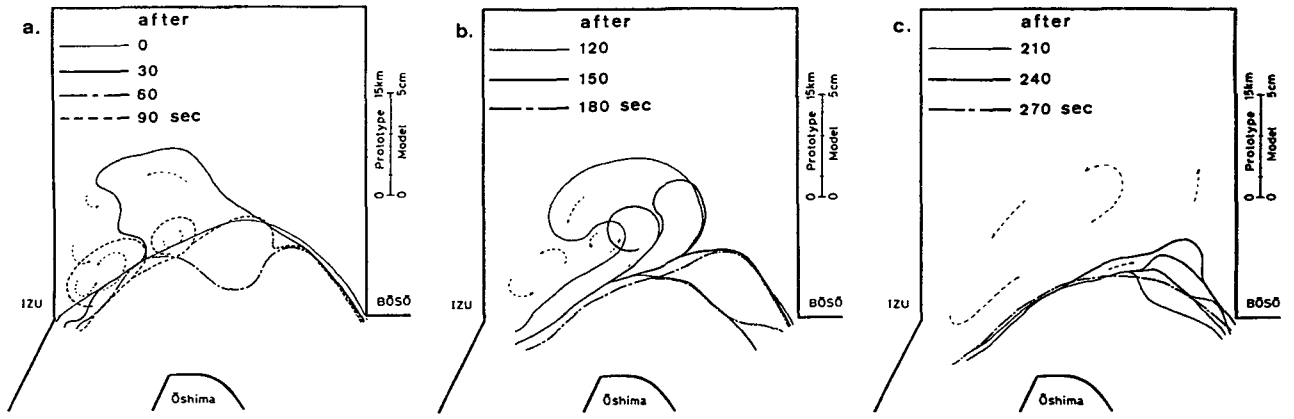

Fig. 4. Variations of the northern boundaries of the flow path (a) from the start of the flow rate increase (Q=5.5→14.0 cc/s) to 90 seconds, (b) from 120 seconds to 180 seconds and (c) from 210 seconds to 270 seconds at intervals of 30 seconds.

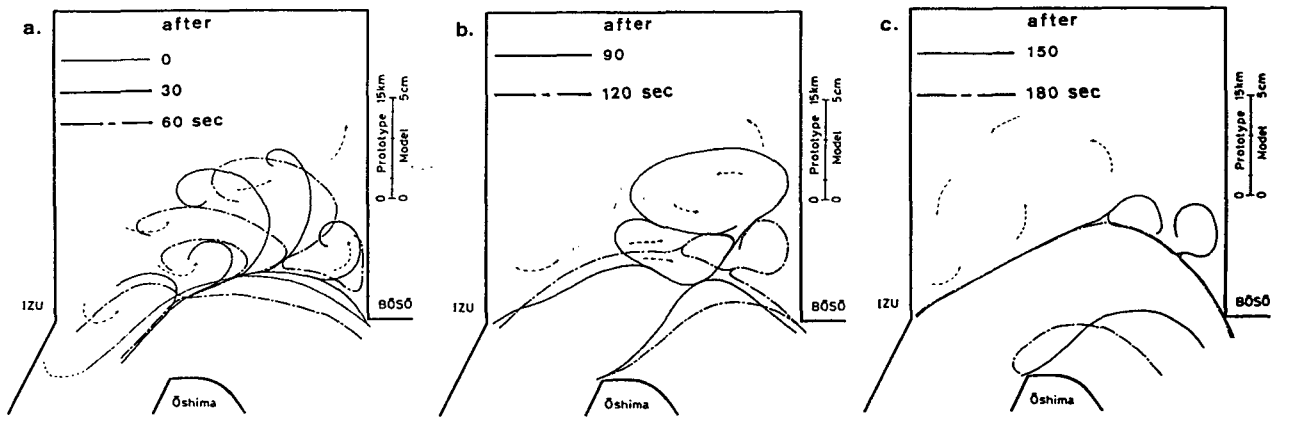

Fig. 5. Variations of the northern boundaries of the flow path (a) from the start of the flow rate decrease (Q=14.0→5.5 cc/s) to 60 seconds, (b) from 90 seconds to 120 seconds and (c) from 150 seconds to 180 seconds at intervals of 30 seconds.

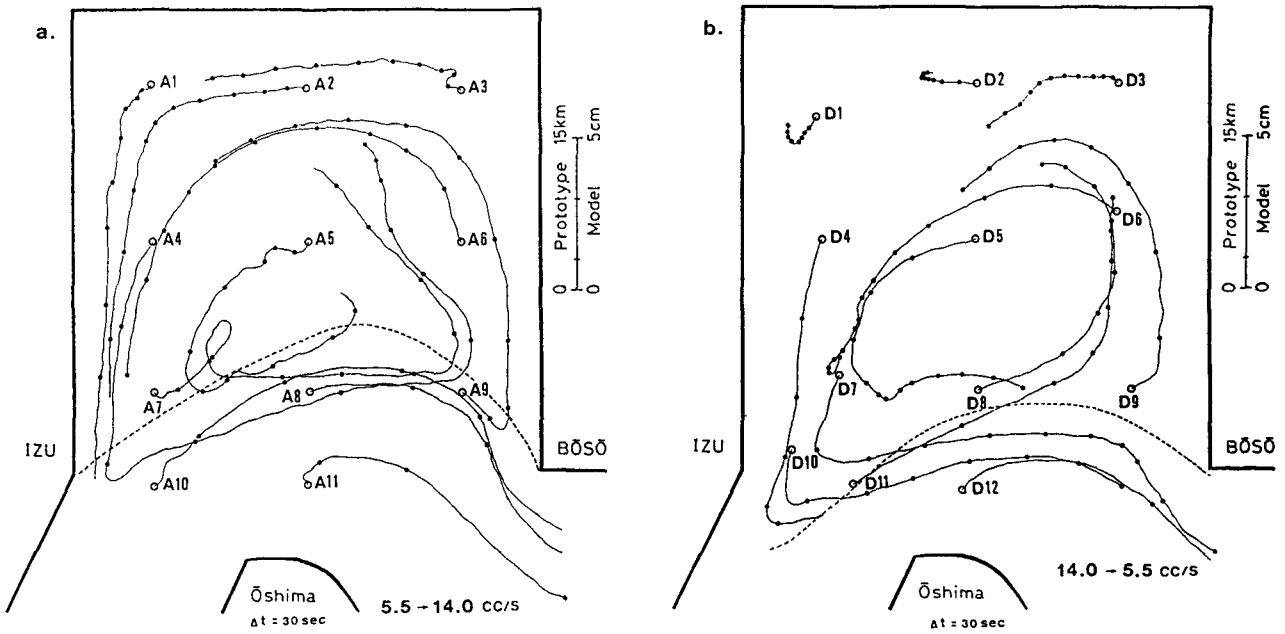

Fig. 6. Trajectories of each fluid particle in the model bay (a) when the flow rate is increased (Q=5.5→14.0 cc/s) and (b) decreased (Q=14.0→5.5 cc/s). Time intervals between successive dots on the trajectory lines at each point indicate 30 seconds.

of the KTF. In the eastern boundary region, the branched flow path and the coastal waters are mixed. 90 seconds later (Fig. 5 (b)), the coastal waters of the cyclonic circulation which are extended southward at the western boundary region and are inserted into the branched flow path move to east gradually and begin to be transformed as eddies. Since then, the eddies grow near the eastern boundary and the northern edge of the KTF goes up north considerably. 120~150 seconds later, the flow path proceeds northward and the mixed waters previously existed on the KTF path flow eastward. 150 seconds later (Fig. 5 (c)), the northern edge of the KTF is little changed.

Water exchange by time variations of volume transport

In order to investigate the behaviour and the exchange of the water mass by flow rate variations, water particles are tracked at 11~12 points in the model bay. Fig. 6 (a) and (b) show the trajectories of each fluid particle when the flow rates are increased and decreased in their range of 5.5 cc/s~14.0 cc/s. Time intervals between successive dots on the trajectory lines are 30 seconds. When the flow rate is increased from 5.5 cc/s to 14.0 cc/s (Fig. 6 (a)), point A7, A8 and A9 flow into the inner part of the bay from the KTF region. Point A7 is dragged into the cyclonic eddies by wakes. Then, it moves to east and flows into the inner side of the bay. Point A4 and A6 which belong to the cyclonic circulation region draw cyclonic trajectories. Point A1, A2 and A3 near the northern boundary flow along the boundary getting on the cyclonic circulation. But point A3 draws a local small anticyclonic trajectory till 60 seconds from the beginning of the flow rate increase. The cyclonic circulation water through Oshima eastern channel was scarcely discharged from the beginning of the flow rate increase till about 300 seconds when the changed flow (Q=14 cc/s) became quasi-steady.

When the flow rate is decreased from 14.0 cc/s to 5.5 cc/s (Fig. 6 (b)), point D4, D5, D7 and D10 in the west of the bay go out through Oshima eastern channel along the KTF path newly formed after the flow rate decrease. Penetration of the KTF into the bay and mixing with the cyclonic circulation are less than those in the case of the flow rate increase. Point D11 and D8, which are located in the frontal region between the KTF and the cyclonic circulation, flow to northeast and mix with the inner cyclonic circulation water. Point D1 and D2 in the north of the bay draw sluggish anticyclonic trajectories since the flow rate has decreased. Point D6 and D9 near the eastern part of the bay go up north with time and circulate with a cyclonic circulation newly formed after the flow rate decrease. In the process of the water exchange, it

is found that the KTF scarcely flows into the bay or mixes with the cyclonic circulation water. However, it is confirmed that the cyclonic circulation water is discharged to the outside of the bay by its southward extension.

Rate of water exchange

Sagami Bay is a deep and open-shaped bay. Also, tidal currents in the bay are very small in deeper regions except continental selves. Meanwhile, it is assumed that the water exchange between the northern inner parts of the bay and the entrance parts of the bay is mostly carried out by fluctuations of the KTF path. Therefore, it is considered that the water exchange in Sagami Bay is generally carried out between the cyclonic circulation water in the inner parts of the bay and the KTF water. In barotropic mode, the expected examples of water exchange are ; 1) water exchange in quasi-steady state by wakes (frontal eddies in baroclinic mode) at the southwestern boundary of the bay near the entrance of the approaching channel, 2) water exchange by the fluctuations of the KTF path and the cyclonic circulation (in baroclinic mode, the frontal eddies and the effect of a coastal boundary density current are included), 3) water exchange by wind driven currents etc.. The rate of the water exchange in quasi-steady state for 1) could be obtained by estimating the amount of the inflow of the KTF into the bay, which is calculated from the relationship $K_h \propto L^2T^{-1}$ if the transfer period T, radius L of a wake and then horizontal eddy viscosity K_h are measured. The water exchanges for 2) and 3) are in non-steady state, so that it is very hard to estimate their substantial amount. However, the overall amount of water exchange in both quasi-steady state and non-steady state was estimated in our experiments.

When the flow rates of the KTF are 5.5 cc/s, 14.0 cc/s and 42.0 cc/s, the volume amount of the bay water Qs containing the cyclonic circulation mostly are 986.15 cc/s, 1210.0 cc/s and 1226.0 cc/s respectively, which are calculated by areas of the model bay. Also the flow amounts P of the KTF which enter into and are added to the cyclonic circulation are 1.44 cc/s, 2.68 cc/s and 7.70cc/s, respectively. Therefore in the case of the water exchange in quasi-steady state, the rates of the water exchange P/Qs are about 0.15%, 0.22% and 0.62%, respectively and its average 0.33%. It is assumed that the water exchange by the fluctuation of the KTF is mainly depended on its fluctuation period and the response time of the bay. However, in our experiments, the flow rate increase of the KTF appeared as a wake at the western boundary of the bay and increased the volume transports of the cyclonic circulation. Then, the increased flow rates from the KTF are completely mixed with the cyclonic circulation water. The flow rate decrease of the KTF caused the cyclonic circulation water to extend southward and the amounts of the decreased cyclonic circulation water discharged through Oshima eastern channel.

Fig. 7 shows variations of the water exchange rates $P/(V_0+P)$ for the flow rate increase 5.5→14.0 cc/s ("Increase") and $P/(V_0-P)$ for the flow rate decrease 14.0→5.5 cc/s ("Decrease"), respectively. Where, P indicates the increased or the decreased flow amounts from the KTF and V_0 total volume transports of the cyclonic circulation in the bay. The rate of the water exchange for the flow rate increase is about 0.1 at $\Delta t/\tau=0.1$ ($\tau=300$ sec), which means that the flow amounts entered into the inner bay from the KTF are equivalent to about

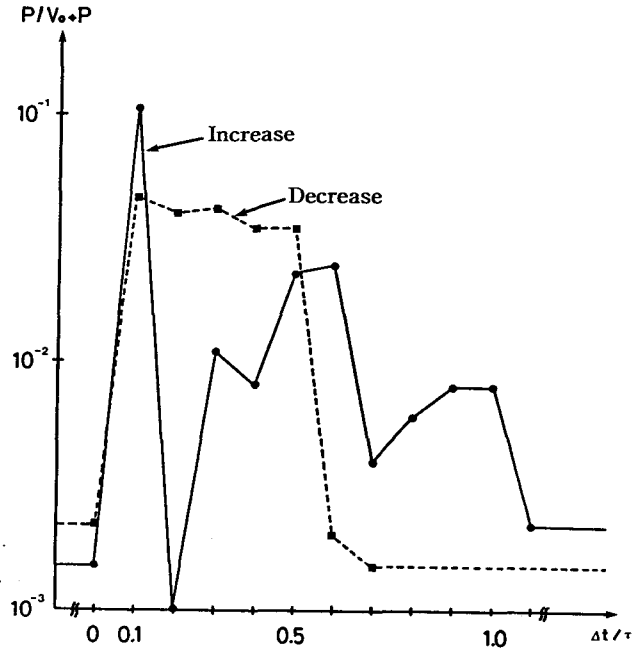

Fig. 7. Variations of the water exchange rates $P/(V_0+P)$ for the flow rate increase 5.5→14.0 cc/s ("Increase" in figure) and $P/(V_0-P)$ for the flow rate decrease 14.0→5.5 cc/s ("Decrease" in figure), respectively. P indicates the increased or the decreased flow amounts and V_0 total volume transports of the cyclonic circulation in the bay.

10% of the total volume transport of the cyclonic circulation within 30 seconds (1.7 days in prototype) after the flow rate increase. Where Δt represents the time lapses (every 30 seconds) from the beginning of the flow rate change and represents the response time (300 seconds) required for the KTF to get to the quasi-steady state of the changed flow rate. Since then, the rate of the water exchange fluctuates from 1.0×10^{-3} to 2.5×10^{-2} and become constant as 2.2×10^{-3} which is the value in quasi-steady state of $\Delta t/\tau>1.0$ when the flow rate increase is completed. The total rate of water exchange is about 0.1 from $\Delta t/\tau=0.1$ to $\Delta t/\tau=0.6$, so that the total flow amounts from the KTF into the inner bay are about 20% ($P/(V_0+P)=0.2$) of all the bay water. The rate of the water exchange for the flow rate decrease is 4.6×10^{-2} at $\Delta t/\tau=0.1$, $3.5\times10^{-2}\sim4.2\times10^{-2}$ at $\Delta t/\tau=0.2\sim0.5$ and 2.2×10^{-3} at the quasi-steady state of $\Delta t/\tau=0$. However, for $\Delta t/\tau>0.7$ the rate of the water exchange is 1.5×10^{-3} that is the value in quasi-steady state when the flow rate decrease is completed, and then shows no change in its value. The total rate of the water exchange is 0.2 from $\Delta t/\tau=0.1$ to $\Delta t/\tau=0.6$, so that the discharged flow amounts of the cyclonic circulation water caused by the flow rate decrease 14.0→5.5 cc/s are equivalent to about 20% ($P/(V_0-P)=0.2$) of all the bay water. These experimental results indicate that the flow amounts entered from the KTF or the discharged flow amounts of the cyclonic circulation water is about 20% of all the bay water during a short-term period fluctuation of the KTF (a flow rate change of 8.5 cc/s within 30 seconds). Therefore, it is assumed that the flow rate changes of the KTF made the water exchange promote, which is due to the non-steady effect for the water exchange in the bay.

Fig. 8 indicates schematic views of the water exchanges between the KTF water and the cyclonic circulation water in the bay and variations of the flow patterns by the flow rate changes. In the upper Fig. 8, the increase of the flow rate makes the flow amounts of the KTF and the vorticity enter into the bay by means of topographical eddies (wakes) at the end of the western boundary of the bay (①~② process of the upper Fig. 8). Then, the flow path advances southward gradually (③ process of the upper Fig. 8) and the cyclonic circulation becomes weaker. On the other hand, the decrease of the flow rate makes the wakes from the western boundary of the bay weak (the lower Fig. 8) and the cyclonic circulation in the inner bay extend to the western entrance of the bay (that is, the increase of the radius of the cyclonic circulation, ①~② process of the lower Fig. 8). Some of the extended cyclonic circulation joins with the KTF and flows out through the Oshima eastern channel along the KTF path after the decrease of the flow rate (③ process of the lower Fig. 8).

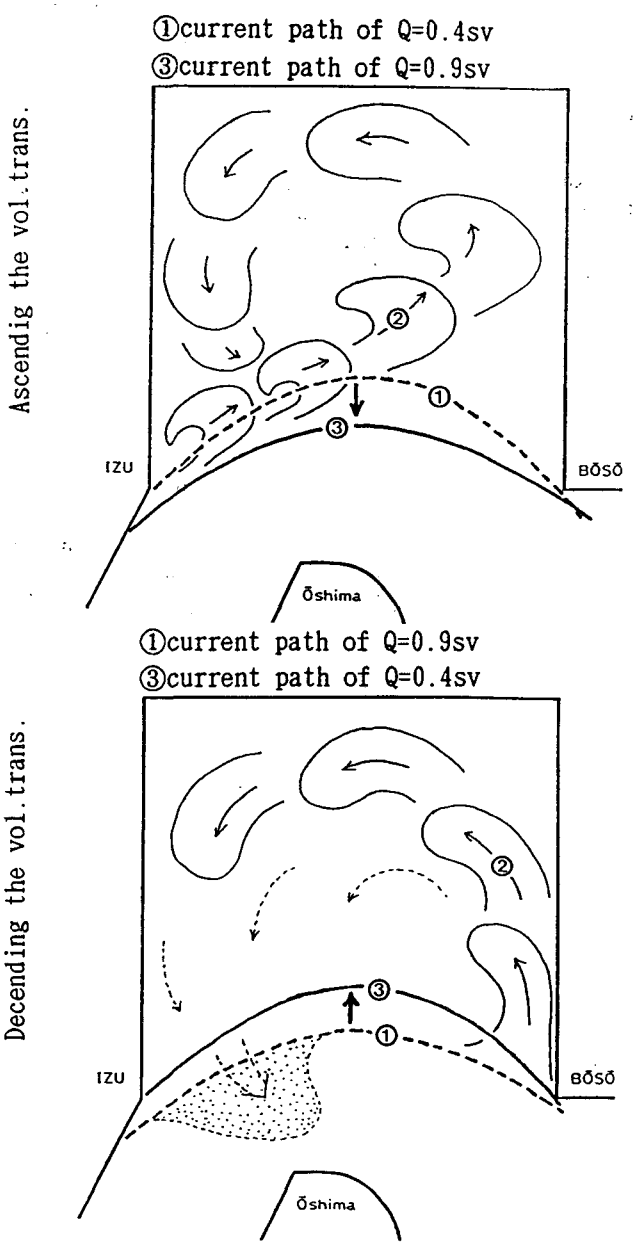

Fig. 8. Schematic views of the water exchanges between the KTF water and the cyclonic circulation water in the bay and variations of the flow patterns by the flow rate changes. The upper and lower figures indicate the case of the flow rate increase and the flow rate decrease, respectively.

References

Choo, H.S. And T. Sugimoto. 1992. Hydraulic model experiment on the circulation in Sagami Bay (1) - Dependency of the circulation pattern on Reynolds and Rossby Numbers in Barotropic rotating model-. Bulletin on Coastal Oceanography, 29, 179~189 (in Japanese).

Choo, H.S. And T. Sugimoto. 1999. Hydraulic model experiment on the circulation in Sagami Bay, Japan (IV) -The time-varying states of the flow pattern and water exchange in baroclinic rotating model-. Bulletin of the Korean Environmental Sciences Society (in press).

Iwata, S. and M. Matsuyama. 1989. Surface circulation in Sagami Bay: the response to variations of the Kuroshio Axis. J. Oceanogr. Soc. Japan, 45, 310~320.

Kawabe, M. and M. Yoneno. 1987. Water and flow variations in Sagami Bay under the influence of the Kuroshio path. J. Oceanogr. Soc. Japan, 43, 283~294.

Kawata, K. and N. Iwata. 1957. Currents in Sagami Wan. Hydrographic Bulletin, Maritime Safety Board, Tokyo, Japan, 53, 44~47 (in Japanese).

Kimura, S., H.S. Choo and T. Sugimoto. 1994. Characteristics of the eddy caused by Izu-Oshima Island and the Kuroshio Branch Current in Sagami Bay, Japan. J. Oceanogr. Soc. Japan, 50, 373~389.

Nakada, H. and K. Hasunuma. 1987. Observation on transport and distribution of fish eggs and larvae. Environment of Fisheries Oceanography, 159~169 (in Japanese).

Nakata, H., K. Hasunuma and T. Hirano. 1989. Distribution of sardine eggs and larvae related to the surface circulation in Sagami Bay. J. Oceanogr. Soc. Japan, 48, 11~23.

Sugimoto, T. and H.S. Choo. 1992. General mechanism of the Kyucho Event (a sudden rapid coastal boundary current) in the coastal area of the Kuroshio. Bulletin on Coastal Oceanography, 30, 45~57 (in Japanese).

Taira, K. And T. Teramoto. 1981. Velocity fluctuations of the Kuroshio near the Izu Ridge and their relationship to current path. Deep-sea Research, 10, 1187~1197.

Taira, K. And T. Teramoto. 1986. Path and volume transport of the Kuroshio current in Sagami Bay and their relationship to cold water masses near Izu Peninsula. J. Oceanogr. Soc. Japan, 42, 212~223.

Tameishi, H. 1988. Fisheries of Saurel and oceanic condition in Sagami Bay. Bull. Japan Soc. Fish. Oceanogr., 52, 319~323 (in Japanese).

Uda, M. 1937. The effect of oceanic and weather conditions on fishing condition during the yellowtail season in Sagami Bay. Fishery Experimental Station, 8, 1~59 (in Japanese).

Whitehead, J.A. and A.R. Miller. 1979. Laboratory simulation of the gyre in the Alboran Sea. J. Geophys. Res., 84, 3733~3742.

Yoshida, S. 1960. On the short period variation of the Kuroshio in the adjacent sea of Izu Islands. Hydrographic Bulletin, Maritime Safety Board, Tokyo, Japan, 65, 1~18 (in Japanese).